

Quantum signatures of the classical topological nonconnectivity threshold

F. Borgonovi,^{1,2} G. L. Celardo,^{1,3} and G. P. Berman³¹*Dipartimento di Matematica e Fisica, Università Cattolica, via Musei 41, 25121 Brescia, Italy*²*I.N.F.N., Sezione di Pavia, Italy*³*Theoretical Division and CNLS, Los Alamos National Laboratory, Los Alamos, New Mexico 87545, USA*

(Received 19 September 2005; published 12 December 2005)

A quantum Heisenberg model with anisotropic coupling and all-to-all interaction has been analyzed using the Bose-Einstein statistics. In F. Borgonovi, G. L. Celardo, M. Maianti, and E. Pedersoli, *J. Stat. Phys.* **116**, 1435 (2004), the existence of a disconnection in the classical phase space has been proved analytically. Such topological disconnection occurs when the energy exceeds a suitable threshold value, called the topological nonconnectivity threshold. We address here the problem of finding quantum signatures of such a threshold. An independent definition of the quantum nonconnectivity threshold, motivated by considerations strictly valid in the quantum regime, is given. We also discuss the dynamical relevance of the quantum border with respect to the quantum magnetic reversal. Contrary to the classical case the magnetization can flip even below the classical threshold through macroscopic quantum tunneling. We evaluate the time scale for magnetic reversal from statistical and spectral properties for a small number of particles and in the semiclassical limit.

DOI: [10.1103/PhysRevB.72.224416](https://doi.org/10.1103/PhysRevB.72.224416)

PACS number(s): 75.10.Jm, 05.30.-d, 75.60.Jk

I. INTRODUCTION

Anisotropic Heisenberg models are characterized by an interesting feature depending on their energy value: below some energy threshold their phase space is topologically divided into two separate branches that cannot be connected by dynamical paths. The existence of such an energy threshold, called at the beginning the nonergodicity threshold,¹ but later^{2,3} the topological nonconnectivity threshold (TNT), has been proved for a class of classical Heisenberg models with anisotropic coupling and infinite range of interaction. Below the TNT the energy surface is disconnected into two components characterized by an opposite sign of the total magnetization. From a dynamical point of view this means that a magnetized sample with a positive magnetization (residing in one component) cannot demagnetize, since no dynamical paths are allowed to reach the other component (with negative magnetization).

Other dynamical consequences of the TNT in classical Heisenberg models with infinite-range coupling have also been investigated.² In particular, it has been shown that above the TNT and in a fully chaotic regime, a time scale for the magnetic reversal—i.e., the time needed for the total magnetization to reverse its direction—can be determined as a random process. Magnetic reversal times also show an exponential growth with the number of spins sharing few peculiarities with standard phase transitions, such as a power-law divergence at the TNT itself.

The existence of this energy border is not limited to the infinite-range coupling case and can be in general related to the anisotropy of the coupling when it induces an easy axis of magnetization, defined by the direction of the magnetization in the minimal-energy configuration of the system. The relation between the TNT and range of the interaction has also been studied,³ introducing an interspin interaction potential decaying as $R^{-\alpha}$, where R is the distance among the spins. Defining r as the ratio of the disconnected portion of the energy range with respect to the total energy range, it has

been proved that, for a d -dimensional system, r tends to zero in the thermodynamic limit for $\alpha > d$ (short range) while it remains finite for $\alpha < d$ (long range).³

The results found in the classical model guided our investigations on the quantum side. We are mainly interested here in the quantum signature of the classical TNT and in its relevance with respect to the quantum reversal time of the magnetic moment.

We consider here an infinite-range interacting system since the explicit expression of the TNT has been obtained in this case only. Despite its unphysical character, magnetic systems can be realized, within modern experimental techniques,⁴ described by Heisenberg-like Hamiltonians with an infinite-range term, which could induce the presence of the TNT. Moreover, when the range of the interaction is of the same order of the size of the system, the all-to-all coupling could be an important first-order approximation in the understanding of their behavior.^{5,6} This could be the case for small systems used in present nanotechnology⁷ or for macroscopic systems with long-range interactions.

We first analyze the spectral properties and we establish the existence of a quantum disconnection threshold in close correspondence with the classical one. An analytical estimate of this quantum threshold is given. We will then study the system from a dynamical point of view, analyzing the time scale for quantum magnetic reversal and comparing the quantum magnetic reversal times with the classical ones.

II. MODEL

We consider a system of N particles of spin l , described by the Hamiltonian

$$\hat{H} = \frac{\eta}{2} \sum_{i=1}^N \sum_{j \neq i} \hat{S}_i^x \hat{S}_j^x - \frac{1}{2} \sum_{i=1}^N \sum_{j \neq i} \hat{S}_i^y \hat{S}_j^y, \quad (1)$$

where $-1 < \eta \leq 1$ is the anisotropy constant. We define

$$\hat{m}_{x,y,z} = 1/N \sum_i \hat{S}_i^{x,y,z}$$

as the components of the total magnetization of the system. Due to the anisotropy of the coupling, the system has an easy axis of the magnetization along the y direction. Quantization of the Hamiltonian follows the standard rules. As in the classical case we fix the modulus of the spins to 1. This can be achieved with an appropriate rescaling of the Planck constant, $\hbar \rightarrow \hbar/|S_i| = 1/\sqrt{l(l+1)}$. With this choice, in the classical limit $l \rightarrow \infty$ ($\hbar \rightarrow 0$), the spin modulus remains equal to 1. Because of the infinite-range nature of the interaction, the Hamiltonian (1) is a completely symmetric operator with respect to particle exchange. It is thus natural to limit ourselves to subspaces of definite symmetry. Specifically, we consider the bosonic case (an ensemble of integer spins), so we will limit our analysis in the subspace of all possible completely symmetric states, with dimension $\mathcal{N} = (N+2l)!/[N!(2l)!]$. This choice reduces considerably the dimension of the Hilbert space, allowing us to extend our analysis further in the classical limit. An important property of the Hamiltonian (1) is its invariance under a π rotation about the z axis: the Hamiltonian commutes with the operator $\exp(i\pi \sum \hat{S}_i^z)$, and its eigenstates can be labeled as odd (−) or even (+) according to whether they change or do not change sign under such rotation.

III. QUANTUM SIGNATURE OF THE TNT

The first aim of our analysis on the quantum system is to assess the quantum signature of the classical disconnection threshold.

Let us review the definition of the classical E_{mt} . The phase space of the system is topologically disconnected below a given energy E_{mt} , which can be obtained as in Ref. 1. From symmetry considerations both positive and negative regions of m_y exist on the same energy surface. Indeed the Hamiltonian is invariant under a rotation of π about the z axis for which $S_i^y \rightarrow -S_i^y$ and $S_i^x \rightarrow -S_i^x$. Switching dynamically from a negative m_y value to a positive one requires, for continuity, to pass through $m_y = 0$. Hence, for all energy values above

$$E_{mt} = \text{Min}[H|m_y = 0]$$

magnetization reversal is possible, while it is not possible below it.

Numerical diagonalization of Eq. (1) gives rise to a quasidegenerate energy spectrum with an energy splitting increasing with the energy E . It is a standard result⁸ that the infinite time average of any quantum operator is zero in presence of a nondegenerate discrete spectrum when its diagonal elements in the energy basis are zero. The operator \hat{m}_y satisfies this condition, and thus the total magnetization along the easy axis can in principle change its sign for any energy. What is physically relevant, of course, is the time scale at which this happens. Such a time scale can be obtained by a detailed study of the energy difference between close eigenstates. Specifically, since the matrix elements of \hat{m}_y are different from zero only between energy eigenstates of different parity, it will be important to study the characteristics of the

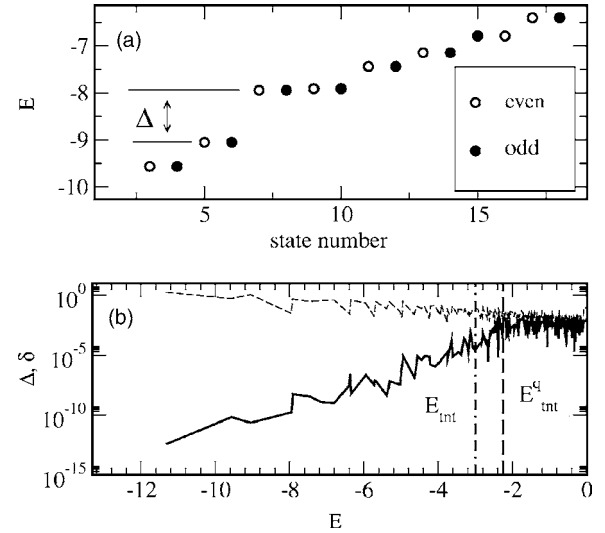


FIG. 1. $N=6$, $l=3$, $\eta=1$. (a) Doublets structure of the low-energy region of the spectrum. The different parity of the states constituting the doublets is shown: solid circles are odd eigenvalues; open circles are even eigenvalues. The energy distance between even and odd eigenvalues is δ . We also indicated the level distance among even eigenstates, Δ (distance between two neighbors, solid circles). (b) The splitting of the doublets, δ , vs the energy E (solid heavy line) and the nearest-neighbor level spacing $\Delta(E)$ (thin dashed line). Also shown as vertical lines: the quantum disconnection border, E_{mt}^q (dashed line), computed analytically from Eq. (4), and E_{mt} (dash-dotted line).

energy distance between even and odd eigenstates. The possibility for the magnetization to reverse its sign also in the energy region where it would be classically forbidden can be interpreted as a manifestation of macroscopic quantum tunneling.⁹ (The total magnetization can be a macroscopic quantity.)

The quantum fingerprint of the classical topological disconnection can be found in the analysis of the energy spectrum, which turns out to be characterized by the presence, in the low-energy region, of quasidegenerate doublets; see Fig. 1(a). Each i th doublet is composed by an even and an odd eigenstate, with energy E_+^i and E_-^i whose difference is given by

$$\delta(E^i) = |E_+^i - E_-^i|. \quad (2)$$

It is also useful to define the spacing between eigenstates of the same parity as

$$\Delta(E^i) = |E_+^{i+1} - E_+^i|. \quad (3)$$

Of course doublets are well defined as soon as $\delta \ll \Delta$. Their behavior as a function of the energy is shown in Fig. 1(b). As one can see, while the distance between eigenenergies of the same parity Δ decreases in a smooth way on increasing the energy, the energy splitting δ changes from an exponential behavior to a constant plateau. From the same figure it is also clear that this happens approximately at the classical energy threshold. This is not surprising if one thinks of the quasidegeneration as an intrinsic feature of the classical topological disconnection. Therefore we may identify, at least numeri-

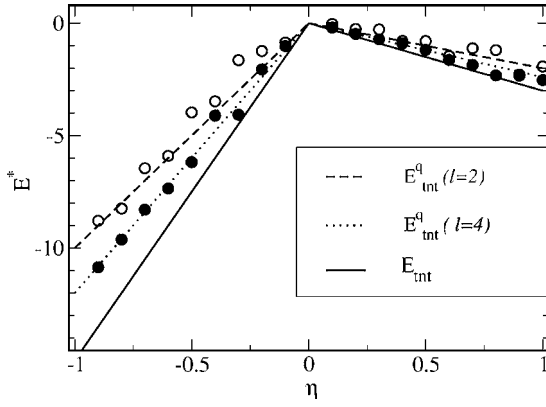


FIG. 2. Comparison between E_{int}^q (lines) and E^* (symbols) for different l values vs η and $N=6$ particles. Open circles stand for E^* and $l=2$. Solid circles stand for E^* and $l=4$. The dashed line represents E_{int}^q for $l=2$. The dotted line is E_{int}^q for $l=4$. Also shown, as the solid line, the classical TNT: E_{int} .

cally, the quantum analog of the classical TNT as the energy at which

$$\delta(E^*) \approx \Delta(E^*).$$

In order to have a meaningful definition, we should require such a quantum threshold to have the appropriate semiclassical limit. The behavior of E^* for different l values as a function of the anisotropic coefficient η is reported in Fig. 2. As one can see $E^* \rightarrow E_{int}$ as l increases, which confirms the soundness of our definition.

Together with the numerical definition we may give an analytical expression of the quantum threshold as a quantum correction to the classical TNT. Indeed, since in the classical case, E_{int} had been obtained¹ computing the minimum of $-(\eta/2)\sum(S_i^x)^2$ when $\eta > 0$ and of $(\eta/2)N^2m_x^2 - (\eta/2)\sum(S_i^x)^2$ when $\eta < 0$, we may assume that the lowest eigenvalues of the corresponding quantum operator could give an analytical estimate of the quantum threshold. Computing the lowest eigenvalue, E_{int}^q , one gets

$$E_{int}^q \sim -\frac{\eta N}{2}(\hbar l)^2 \quad \text{for } \eta > 0,$$

$$E_{int}^q \sim \frac{\eta N}{2}(N-1)(\hbar l)^2 \quad \text{for } \eta < 0. \quad (4)$$

Of course, the question arises if the two definitions of quantum threshold are equivalent. The nice agreement between the numerical values E^* and our analytical estimate E_{int}^q presented in Fig. 2 (compare symbols with lines) shows that this is the case.

The exponential behavior of the level splittings δ with the energy is generally characterized by wide fluctuations. Therefore, it is convenient to perform a suitable average over a small energy bin. This allows us to understand in greater detail how the semiclassical limit is recovered in terms of spectral properties.

As shown in Fig. 3, on increasing the semiclassical pa-

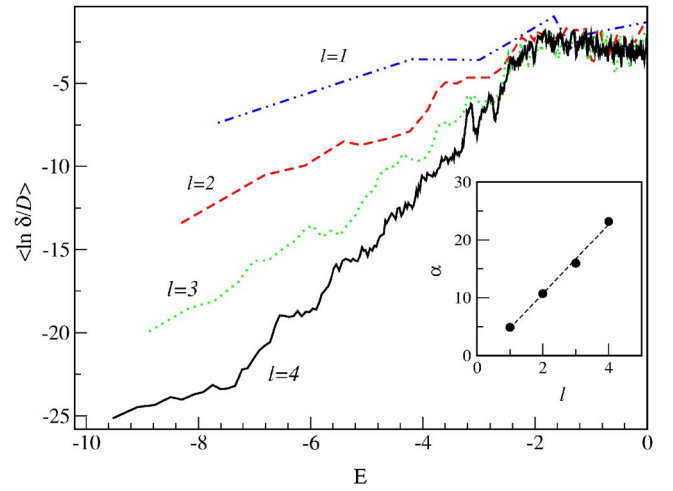


FIG. 3. (Color online) Average (over energy bins) of $\langle \ln(\delta/D) \rangle$ vs the energy E , for $N=6$, $\eta=1$, and different l values: $l=1$: dash-dotted (blue) line, $l=2$: dashed (red) line, $l=3$: dotted (green) line, and $l=4$: heavy (black) line. Here D is the average level spacing. Inset: the linear dependence of the slopes α obtained from the exponential fit. A linear fit gives $\alpha = -1.3 + 6l$.

rameter l , the (exponential) rate of growth becomes the steepest. Linear fits allow us to extract the value of the exponent α , obtained from the standard regression $\langle \ln(\delta) \rangle = \alpha E + C$. It turns out that α depends linearly on the semiclassical parameters l , as shown in the inset of Fig. 3. That way the classical picture is recovered since, when $l \rightarrow \infty$, $\delta(E) \approx 0$ for $E < E_{int}$.

For $E > E_{int}$ level splittings for systems with different l values have generally different average values. Normalizing them with respect to the average energy spacing

$$D = \frac{\text{size of the energy spectrum}}{\text{total number of levels}}$$

allows us to get the same plateau in the semiclassical limit.

Although a detailed study of the differences between the mean-field single-spin model usually used in literature^{9,10} and our many-spin model will be presented elsewhere,¹¹ the two models differ substantially. Let us consider, for instance, the mean-field approximation of our Hamiltonian (1), in a similar way as what has been done for the classical model:²

$$H_{mf} = \frac{\eta}{2} N^2 m_x^2 - N^2 m_y^2; \quad (5)$$

then, for $\eta > 0$, the classical TNT is zero for the mean-field model while is equal to $-\eta/2$ for Hamiltonian (1). This clearly shows how different the two models can be.

IV. TIME SCALE FOR MAGNETIC REVERSAL

Let us now analyze the time scale for magnetic reversal in the quantum system, comparing the results with the classical ones.² Since in the classical case the reversal times have been determined at a fixed energy (microcanonical approach), we adopt here the same procedure and compute the reversal time

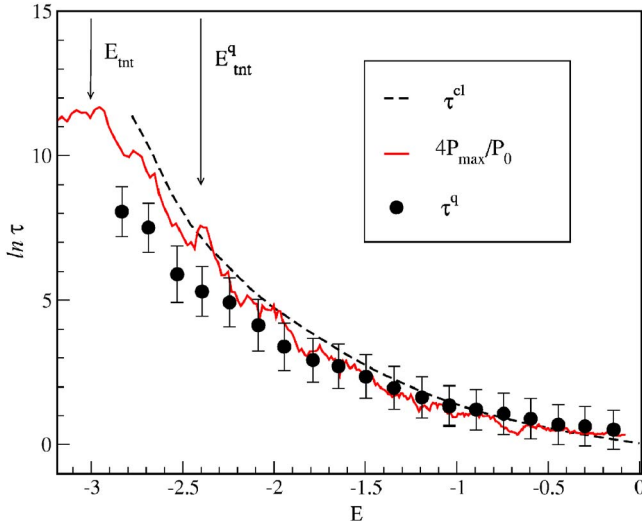


FIG. 4. (Color online) The quantum average reversal time τ^q (circles) as a function of E is shown for the case $N=6$, $\eta=1$, and $l=4$ and is compared with the classical one (dashed black line), showing good agreement above E_{tnt}^q and a deviation near E_{tnt} (both indicated as vertical arrows). Also shown, as a solid (red) line, $4P_{\text{max}}/P_0$ averaged over close eigenfunctions.

of the quantum average magnetization starting from an ensemble of initial states, $|\psi\rangle$, obtained choosing randomly energy eigenstates in a narrow energy interval $|\psi\rangle = \sum_E^{E+\Delta E} C_E |E\rangle$. The coefficients C_E have been randomly chosen in modulus and phase and such that $\sum_E^{E+\Delta E} |C_E|^2 = 1$. Since the total magnetization along the easy axis, \hat{m}_y , connects only energy eigenstates with different parity, we have

$$\langle m_y(t) \rangle = 2 \left\{ \text{Re} \sum_{E_+, E_- = E}^{E+\Delta E} C_{E_+}^* C_{E_-} e^{-it/T} \langle E_+ | \hat{m}_y | E_- \rangle \right\}, \quad (6)$$

where $T = \hbar/(E_- - E_+)$. From $\langle m_y(t) \rangle$ we compute the time of first passage through zero for each initial state of the ensemble. From these times we obtain the average magnetic reversal time τ^q . Before presenting the results of our analysis let us recall that in the quantum case, at variance with the classical one, it is legitimate to ask what is the time scale for magnetic reversal in the whole energy range. Indeed, since the energy spectrum is nondegenerate, from Eq. (6), the average magnetization will soon or later reverse its sign, even below the TNT.

Quantum (and classical) magnetic reversal times versus energy in the region above E_{tnt}^q are shown in Fig. 4. As one can see there is good agreement between classical and quantum times. Note that the classical times diverge at E_{tnt} , at variance with the quantum ones which are systematically smaller, in the region between E_{tnt} and E_{tnt}^q . This is not surprising since the possibility of tunneling will enhance the probability for the magnetization to reverse its sign.

In the classical case² we successfully evaluated the reversal times from the entropic barrier, ΔS , between the most probable value of the magnetization and its zero value, $\tau \sim e^{-\Delta S} = P_{\text{max}}/P_0$. Following the classical case we also computed P_{max}/P_0 from the quantum probability distribution of

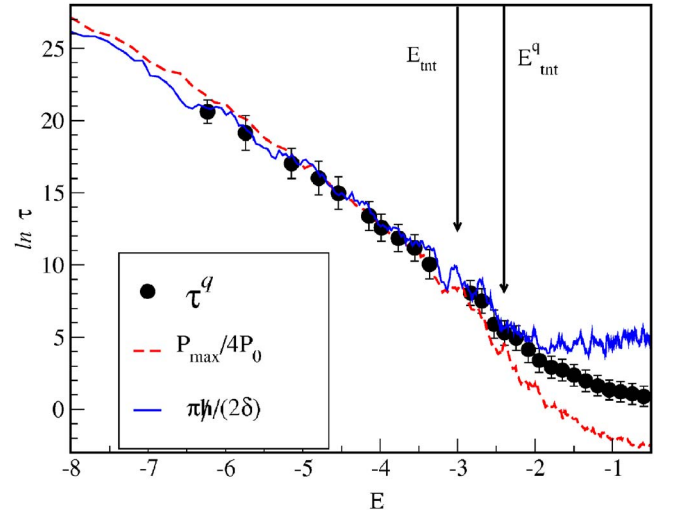


FIG. 5. (Color online) Comparison between dynamical and tunneling splittings in the classically forbidden energy region. Circles: dynamical quantum reversal times. Solid (blue) line: tunneling splittings $\tau^q \sim \pi\hbar/(2\delta)$ for the case $N=6$, $l=4$. Dashed (red) line: $P_{\text{max}}/4P_0$. Vertical arrows indicate classical and quantum thresholds.

the magnetization, $P(m_y)$, and compared the dynamical times τ^q with the probabilistic ones given by cP_{max}/P_0 , where c is a constant. As one can see from Fig. 4 the agreement between probabilistic and dynamical times is fairly good where classical and quantum times agree, while is less accurate in the crossover region, between E_{tnt} and E_{tnt}^q .

Let us now discuss, in detail, the behavior of the quantum reversal times below E_{tnt}^q . In the low-energy region of the spectrum, due to the intrinsic quasidegeneracy, the dynamics can be entirely characterized by the energy difference δ . This occurs if the energy bin ΔE of the initial state is sufficiently small so that one single doublet belongs to it. The dynamics is thus oscillatory with a period given by $2\pi\hbar/\delta$. Indeed, under this condition, the magnetization oscillates coherently between states with opposite sign, a phenomenon known as macroscopic quantum coherence.¹⁰ This period also represents, within a numerical factor, the time for the first passage to zero of $\langle m_y(t) \rangle$. One thus can assume

$$\tau^q \sim \pi\hbar/(2\delta).$$

The agreement, over many orders of magnitude, is shown in Fig. 5. Also, below E_{tnt}^q , we checked the proportionality of the reversal times with P_{max}/P_0 . It is quite surprising that P_{max}/P_0 turns out to be proportional to the tunneling rates and then, when properly defined, to the reversal times, even in the region classically forbidden (below E_{tnt}) where the only mechanism allowing the jumping of the barrier is through macroscopic quantum tunneling; see Fig. 5. This suggests that the mechanism producing this proportionality can also have a nonclassical origin. One should also note that the constant of proportionality is different below E_{tnt} and above E_{tnt}^q . This explains the poor agreement between the statistical and dynamical times in the crossover region ($E_{\text{tnt}} < E < E_{\text{tnt}}^q$).

From the results presented here we can address the problem of the dynamical signature of the classical TNT. In the semiclassical limit the crossover region becomes very narrow ($E_{mt}^q \rightarrow E_{mt}$); thus, we can expect a crossover of the reversal time from a power law, like in the classical case,² to an exponential. Moreover, Fig. 3 suggests how the classical limit is recovered: indeed $\delta \approx 0$ as $l \rightarrow \infty$, for energies below E_{mt} , which is consistent with the fact that the magnetization cannot reverse its sign below E_{mt} in the classical system.

V. CONCLUSION

In conclusion we have found a quantum signature of the classical TNT in the spectral properties of the system leading to the definition of a quantum disconnection threshold, E_{mt}^q , with the correct classical limit. Below E_{mt}^q the spectrum is characterized by the presence of quasidegenerate doublets, whose energy difference $\delta(E)$ depends exponentially on E . The quantum reversal times of the total magnetization have been studied and compared with the classical ones above E_{mt} . We have also shown that the total magnetization can flip in the energy region classically forbidden. Quite surprisingly, quantum reversal times (and thus the tunneling rates) are still proportional to P_{max}/P_0 even below E_{mt} .

The existence of the classical TNT allows us to address an energy region where to look for macroscopic quantum phe-

nomena, which have recently raised much interest.¹² Indeed the fact that the total magnetization can reverse its sign even below the TNT can be seen as a manifestation of macroscopic quantum tunneling, a well-known phenomenon in micromagnetism, also found experimentally.^{13,14} Nevertheless, macroscopic quantum tunneling of magnetization arises in the literature,^{9,10} from phenomenological single-spin Hamiltonians, where the single spin describes the total magnetic moment of the system, and no reference to the range of the interaction has been explicitly pointed out. On the other hand, we presented here a many-particle system in which this phenomenon clearly arises, in connection with the existence of the disconnection border and with the long-range nature of the interaction.

Let us notice that while in this paper we consider the case where the ground state is determined by a ferromagnetic coupling among the spins, it would be interesting to study the case with an antiferromagnetic ground state¹⁵ to see if the TNT could be found also in that case.

ACKNOWLEDGMENT

G.L.C. acknowledges financial support from LANL and Università Cattolica under the program “Foreign specialization studies.”

¹F. Borgonovi, G. L. Celardo, M. Maiani, and E. Pedersoli, J. Stat. Phys. **116**, 1435 (2004).

²G. L. Celardo, J. Barre, F. Borgonovi, and S. Ruffo, cond-mat/0410119 (unpublished).

³F. Borgonovi, G. L. Celardo, A. Musesti, R. Trasarti-Battistoni, and P. Vachal, cond-mat/0505209 (unpublished).

⁴L. Q. English, M. Sato, and A. J. Sievers, Phys. Rev. B **67**, 024403 (2003); M. Sato, L. Q. English, B. E. Hubbard, and A. J. Sievers, J. Appl. Phys. **91**, 8676 (2002).

⁵D. H. E. Gross, *Microcanonical Thermodynamics: Phase Transitions in Small Systems*, Lecture Notes in Physics Vol. 66 (World Scientific, Singapore, 2001).

⁶*Dynamics and Thermodynamics of Systems with Long Range Interactions*, edited by T. Dauxois, S. Ruffo, E. Arimondo, and M. Wilkens, Lecture Notes in Physics Vol. 602 (Springer, Berlin, 2002).

⁷F. Luis, J. Campo, J. Gomez, G. J. McIntyre, J. Luzon, and D. Ruiz-Molina, cond-mat/0508627 (unpublished).

⁸M. Toda, R. Kubo, and N. Saito, *Statistical Mechanics* (Springer-Verlag, Berlin, 1995), Vol. I.

⁹E. M. Chudnovsky and J. Tejada, *Macroscopic Quantum Tunneling of the Magnetic Moment* (Cambridge University Press, Cambridge, England, 1998).

¹⁰S. Takagi, *Macroscopic Quantum Tunneling* (Cambridge University Press, Cambridge, England, 1997).

¹¹F. Borgonovi, G. L. Celardo, and R. Trasarti-Battistoni, cond-mat/0510079 (unpublished).

¹²A. J. Leggett and A. Garg, Phys. Rev. Lett. **54**, 857 (1985); A. J. Leggett, J. Phys. A **14**, R415 (2002); Rev. Mod. Phys. **59**, 1 (1987).

¹³W. Wernsdorfer and R. Sessoli, Science **284**, 133 (1999).

¹⁴L. Thomas, F. Lioni, R. Ballou, D. Gatteschi, R. Sessoli, and B. Barbara, Nature (London) **383**, 145 (1996).

¹⁵C. Schroder, H.-J. Schmidt, J. Schnack, and M. Luban, Phys. Rev. Lett. **94**, 207203 (2005); H.-J. Schmidt and M. Luban, J. Phys. A **36**, 6351 (2003).